

## Article

# Energy Simulations of a Building Insulated with a Hemp-Lime Composite with Different Wall and Node Variants

Przemysław Brzyski <sup>1,\*</sup>, Magdalena Grudzińska <sup>1,\*</sup>, Martin Böhm <sup>2</sup> and Grzegorz Łagód <sup>3</sup>

<sup>1</sup> Faculty of Civil Engineering and Architecture, Lublin University of Technology, 40 Nadbystrzycka St., 20-618 Lublin, Poland

<sup>2</sup> Faculty of Civil Engineering, Czech Technical University in Prague, Thákurova 7, 166 29 Prague 6, Czech Republic

<sup>3</sup> Faculty of Environmental Engineering, Lublin University of Technology, Nadbystrzycka 40B, 20-618 Lublin, Poland

\* Correspondence: p.brzyski@pollub.pl (P.B.); m.grudzinska@pollub.pl (M.G.); Tel.: +48-815384448 (P.B.); +48-815384448 (M.G.)

**Abstract:** Thermal bridges constitute a significant share in the overall heat losses through building partitions. This is an important issue not only in traditional but also ecological buildings, where the load-bearing structure is often a wooden frame. In partitions insulated with hemp-lime composite, the skeleton is usually hidden in the insulation. However, in some nodes or jambs, wooden elements may be exposed or have a large cross-section, intensifying the heat transfer. This work presents simulations of energy demand in a single-family building insulated with hemp-lime composite, using the BSim dynamic simulation program. The calculations take into account the linear thermal transmittance of structural nodes modeled in the THERM program. The energy demand for heating and the share of thermal bridges in the heat loss of the entire building were calculated for different locations of the structural framework in the walls, as well as the size and number of windows. The share of thermal bridges in heat losses was about 10%, and the differences in energy demand for heating using various frame locations in the wall were negligible.

**Keywords:** hemp-lime composite; thermal bridge; energy demand; building partition; structural node



**Citation:** Brzyski, P.; Grudzińska, M.; Böhm, M.; Łagód, G. Energy Simulations of a Building Insulated with a Hemp-Lime Composite with Different Wall and Node Variants. *Energies* **2022**, *15*, 7678. <https://doi.org/10.3390/en15207678>

Academic Editor: Elena Lucchi

Received: 31 August 2022

Accepted: 14 October 2022

Published: 18 October 2022

**Publisher's Note:** MDPI stays neutral with regard to jurisdictional claims in published maps and institutional affiliations.



**Copyright:** © 2022 by the authors. Licensee MDPI, Basel, Switzerland. This article is an open access article distributed under the terms and conditions of the Creative Commons Attribution (CC BY) license (<https://creativecommons.org/licenses/by/4.0/>).

## 1. Introduction

The aim of the sustainable development policy pursued by the European Union (EU) is to reduce greenhouse gas emissions, including in the construction sector, which accounts for nearly 40% of world energy consumption [1] and about a third of global CO<sub>2</sub> emissions [2]. The EU policy aims to improve the energy efficiency of buildings by around 30% by 2030 [3]. One factor that contributes to the increased energy consumption in the use phase of a building is thermal bridges, which are sometimes difficult to avoid, mainly due to improperly constructed nodes in the building envelope.

Thermal bridges occur mainly in places where various building elements with different thermal parameters are connected, or where the continuity of the insulation is broken. Examples of the occurrence are, among others, the connection of a roof and external wall, the placement of facade and roof windows and external doors, the connection of a balcony with a ceiling, rims, and lintels, and the connection of a foundation wall with a floor on the ground and an external wall. To minimize the presence of thermal bridges, the continuity of the insulation should be maintained along the building envelope [4]. A seamless connection of the floor, wall, and roof thermal insulation should be designed. In the case of insulating wall blocks, the mortar used as a joint can have a large influence on the heat loss [5].

In the area of thermal bridges, such as the corners of external walls, there is a greater thermal phase lag and thermal amplitude than in the rest of the wall [6]. Properly insulating the window-wall connection can also significantly minimize the heat transfer through this

linear thermal bridge [7]. Unfortunately, windows are often installed in the wrong way in terms of maintaining the continuity of insulation [8].

The result of the occurrence of thermal bridges is uncontrolled heat loss during winter, as a result of which large energy losses take place, adversely affecting the thermal balance of the building. In this case, the cost of heating the room increases significantly (compared to a properly insulated building). In addition, in these places, during the summer period, there is an excessive flow of heat into the interior of the building [9,10]. According to one of the studies, thermal bridges in the building envelope may increase the annual energy demand for space heating by 13–42% [11–15].

Another negative effect of the occurrence of thermal bridges in the partitions is the cooling of their internal surface, which may lead to dampness as a result of surface condensation [16,17]. Maintaining a high level of humidity for a long period promotes the development of biological corrosion [18]. Ilomets et al. [19] investigated the possibility of mold occurrence at the location of thermal bridges on the surface of concrete and wooden walls with similar thermal resistance, at an increased relative humidity of internal air. The possibility of mold occurrence on a concrete wall was 54%, and 46% on a wooden wall. Mold or various types of fungi negatively affect the microclimate and, consequently, the health of the inhabitants, as they can release toxic substances. They can contribute to the development or aggravation of allergies and cause rheumatic diseases or diseases of the respiratory system [20–22].

Building materials based on components of plant origin, such as hemp shives, which are used as a filler in an insulation material such as a hemp-lime composite, are particularly sensitive to the destruction caused by biological corrosion in long-term unfavorable humidity conditions [23,24]. The presence of a highly alkaline lime binder has a protective effect, but prolonged contact with water and temperature conditions favorable to mold may cause corrosive processes. Nevertheless, hemp-lime is a moisture-buffering material which stabilizes indoor humidity conditions in the rooms, which also reduces the risk of mold growth on the walls and improves the comfort of living [25]. In the technology of buildings insulated with a hemp-lime composite, the wooden structure is also exposed to the negative effects of thermal bridges. Wood is characterized by a low coefficient of thermal conductivity, about  $0.16 \text{ W}/(\text{m}\cdot\text{K})$  [26] (although about twice as high as composite insulation), and unlike concrete elements, wooden elements are negligible thermal bridges. However, in some construction nodes, there is a need to use increased wooden cross-sections, and the heat transfer coefficient will consequently increase in these areas [27,28].

The thermal bridge can also damage the structure. Temperature differences in adjoining building elements can cause cracks and scratches. If condensation appears, damage may occur at negative temperatures due to the increased stresses caused by the increased volume of freezing water in the capillary pores of the material.

Summarizing the above, the disadvantages of the thermal bridge occurrence in construction are well recognized. However, the characteristics of building partitions with a wooden frame as a load-bearing structure filled with insulation material cause some difficulties in the evaluation of the influence of construction joints on the energy demand in a building. The external walls in such cases may be assembled in two ways: with the construction frame located centrally in relation to wall thickness, or located on the inner side of the wall. Both types of partitions have the same thermal transmittance coefficient ( $U$ ) if the materials of the same type and thickness are used. Nevertheless, the construction joints may show different linear thermal transmittance ( $\psi$ ) values, depending on the location of the timber frame and the area of wooden elements in contact with internal air [27,28]. For instance, external wall corners, a connection of the floor on the ground with external walls, and a connection of a roof with external walls gave smaller heat losses in the case of the central location of the load-bearing frame [27,28]. In the other case (load bearing frame on the inner side of the wall), the joints such as a connection of walls and a ceiling and a window placement in walls demonstrated the smaller  $\psi$  values.

These properties caused the choice of the construction of the walls to not be obvious and the final energy demand to be connected with the types of thermal bridges together with their length. The mentioned issues concerning the partitions with a wooden frame were not investigated in the literature before, and the presented paper is intended to fill this gap with some initial analyses on the subject.

This article presents simulations of heat losses taking into account the influence of linear thermal bridges in a building with two types of external partitions insulated with a hemp-lime composite in Polish climatic conditions. Different variants of walls and structural nodes that had already been presented in [27,28] were considered. For the current work, the remaining thermal bridges in the building were modeled and their linear thermal transmittance coefficients were calculated. The length of most construction joints is strictly dependent on the geometry of the building. However, the perimeter of windows may vary independently from the walls' dimensions. To check if this specific node may change the recommended wall type, three windows of different sizes were taken into account in the simulations. Thermal parameters of composites used in the studies were taken from our own laboratory tests.

## 2. Materials and Methods

### 2.1. Materials Used in Calculations

In the analyzed single-family building, the external walls, roof, and ground floor were insulated with a hemp-lime composite. The calculations used composites tested in other own works [27,28]. The binder of these composites was based on hydrated lime (75% wt.), metakaolin (15% wt.), and gypsum (10% wt.). Table 1 contains data on hemp-lime mixtures used in external partitions.

**Table 1.** Recipes of hemp–lime mixes (weight ratio), apparent density, and thermal conductivity of the tested composites.

Composite Symbol	Binder: Hemp Shives Ratio	Binder: Water Ratio	Apparent Density [kg/m <sup>3</sup> ]	Thermal Conductivity Coefficient [W/(m·K)]	Standard Deviation [W/(m·K)]
Floor mix	2.1:1	1:1.35	627.5	0.112	±0.005
Roof mix	1:1	1:1.5	238.0	0.065	±0.002
Wall mix	1.4:1	1:1.45	362.5	0.080	±0.002

In many publications one can find the results of research on the thermal conductivity coefficient of the hemp-lime composite [29–31]. However, the authors, conducting and continuing many years of research related to this material, decided to use their own results in these calculations. Many factors, for example the type of shives used, have a great influence on the results [32–35]. The authors use shives of local origin in their research (Podlaskie Konopie, Białystok, Poland).

### 2.2. Building and Junctions Used in Calculations

The analyses concern a single-family, two-story house made of lime and hemp technology, with 133.5 m<sup>2</sup> of usable space. Figures 1 and 2 show schematic plans and a cross-section of the building, respectively.

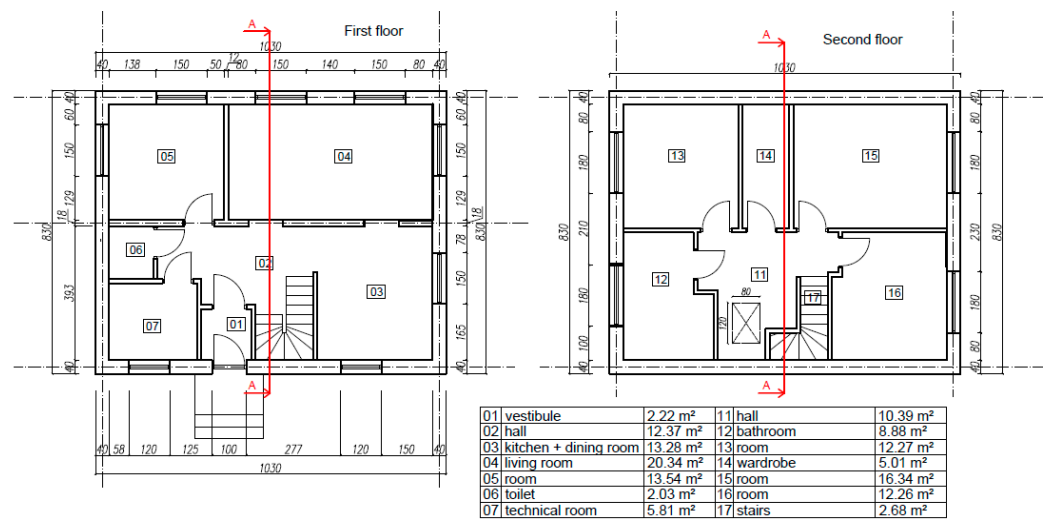


**Figure 1.** Schematic plan of the ground floor and the attic of the analyzed building (A–A means vertical section line).

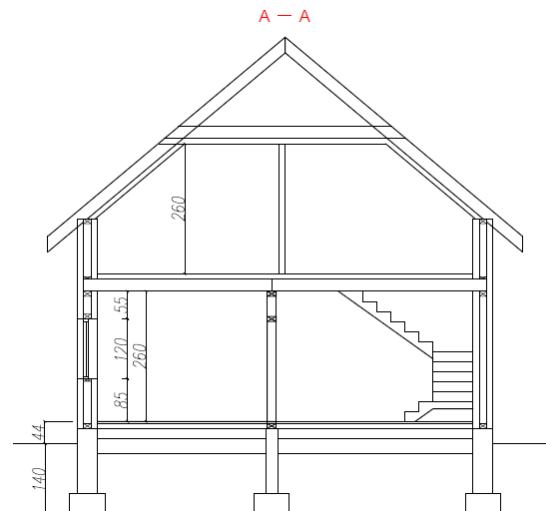


**Figure 2.** Schematic vertical section (A–A) of the analyzed building.

The calculations used the solutions analyzed in our previous works [27,28], and the remaining linear thermal bridges (connection of roof with knee and gable wall) were calculated especially for this study. External walls were assumed to have a timber frame positioned centrally in relation to the wall thickness and in the second case on the internal side of the wall. Both types of walls were insulated with a hemp-lime composite layer 400 mm thick, fulfilling the current requirements in Poland concerning the thermal transmittance coefficient ( $U \leq 0.20 \text{ W}/(\text{m}^2 \cdot \text{K})$ ). Diagrams of the analyzed junctions are shown in Figures 3–8. These solutions are commonly used in practice, so only one type of each of the nodes was used.

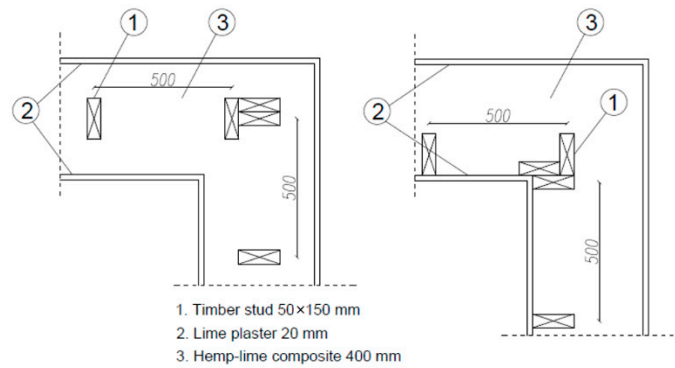


**Figure 3.** External corners with the timber frame located centrally in relation to wall thickness (on the left) and located on the inner side of the wall (on the right).

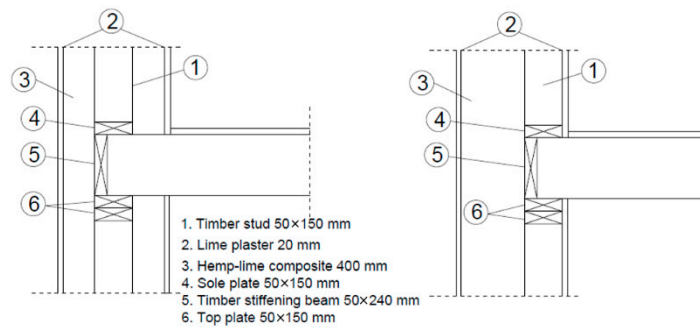


**Figure 4.** Connection of the wall and ceiling in two cases: with the timber frame located centrally in relation to the wall thickness (on the left) and located on the inner side of the wall (on the right).

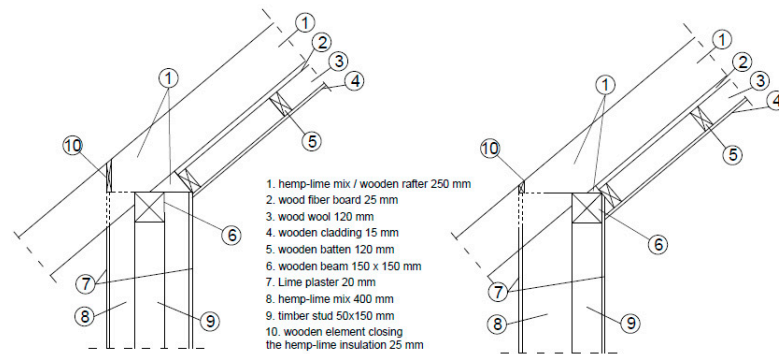


**Figure 5.** Connection of the wall and roof in two cases: with the timber frame located centrally in relation to the wall thickness (on the left) and located on the inner side of the wall (on the right).

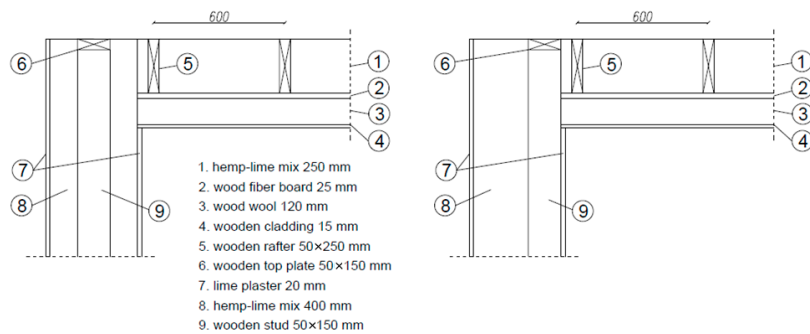


**Figure 6.** Connection of the gable wall and roof in two cases: with the timber frame located centrally in relation to the wall thickness (on the left) and located on the inner side of the wall (on the right).

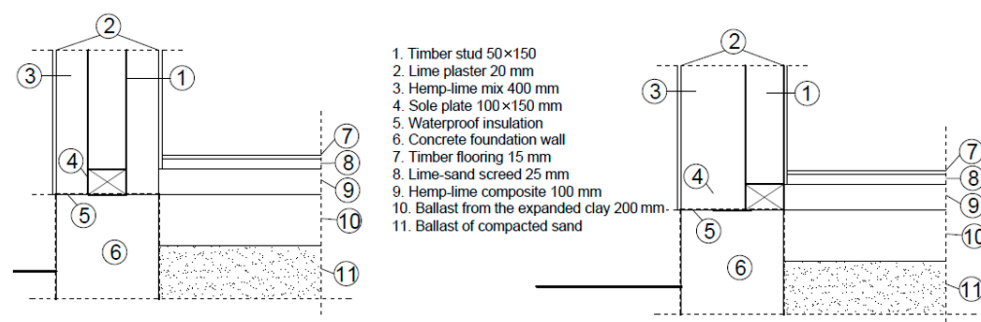


**Figure 7.** Connection of the wall and ground floor in two cases: with the timber frame located centrally in relation to the wall thickness (on the left) and located on the inner side of the wall (on the right).

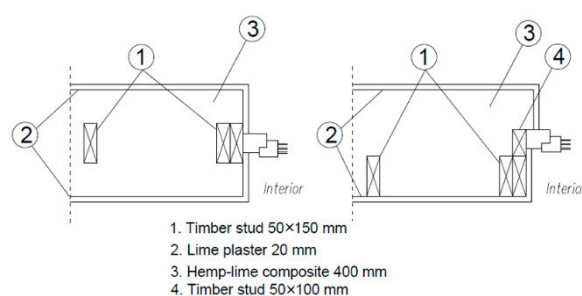


**Figure 8.** Window placement in the wall in the cases: with the timber frame located centrally in relation to the wall thickness (on the left) and located on the inner side of the wall (on the right).

### 2.3. Modelling of the Thermal Bridges

The linear thermal transmittance coefficients ( $\psi$ ) of thermal bridges included in the model were calculated according to the ISO 10211 algorithms [36]. The analyses were based on the stationary, two-dimensional heat transfer and used the THERM program (V 7.6.1.0, Lawrence Berkeley National Laboratory, Berkeley [37]) to determine the temperature field in the nodes. Details on modeling assumptions can be found in publications [27,28]. Thermal properties of materials and elements used in modelling together with boundary conditions are compiled in Tables 2 and 3. Lambda values of materials other than hemp-lime were acquired from ISO 10456 standard [26]. The estimated error energy norm (related to the gradient of heat flux) of the models did not exceed 5% in any of the cases.

**Table 2.** Thermal properties of main materials and elements.

Building Material/Element	Thermal Properties
Hemp-lime mix (wall)	$\lambda = 0.08 \text{ W}/(\text{m}\cdot\text{K})$
Hemp-lime mix (floor)	$\lambda = 0.065 \text{ W}/(\text{m}\cdot\text{K})$
Timber construction element	$\lambda = 0.16 \text{ W}/(\text{m}\cdot\text{K})$
OSB board	$\lambda = 0.13 \text{ W}/(\text{m}\cdot\text{K})$
Lime plaster	$\lambda = 0.70 \text{ W}/(\text{m}\cdot\text{K})$
Gravelite	$\lambda = 0.1 \text{ W}/(\text{m}\cdot\text{K})$
Concrete	$\lambda = 1.3 \text{ W}/(\text{m}\cdot\text{K})$

**Table 3.** Boundary conditions adopted in modelling.

Surface	Temperature	Surface Resistance	Description
Internal	+21 °C	0.13 (m <sup>2</sup> ·K)/W	Heat flow horizontal, simplified *
Internal	+21 °C	0.10 (m <sup>2</sup> ·K)/W	Heat flow upwards, simplified *
Internal	+21 °C	0.17 (m <sup>2</sup> ·K)/W	Heat flow downwards, simplified *
External	−18 °C	0.04 (m <sup>2</sup> ·K)/W	Simplified *
Cut-off planes	-	-	Adiabatic

\* The simplified model means that convective and radiative heat exchange is described by one common surface resistance.

For bridges such as external corners, connections of walls and ceilings, and connections of roofs and knee or gable walls, the values of the linear thermal transmittance coefficients were fixed. These joints are usually constructed in a typical way, and therefore the values of the  $\psi$  factors were not expected to change significantly. For the remaining joints (connection of walls and a ground floor, window placement in external walls) the best case of the linear thermal transmittance coefficients (based on previous research) was taken into account in the current analyses [27,28]. The lengths of the particular bridges together with their  $\psi$  values are gathered in Table 4.

**Table 4.** Diagrams of the bridges modeled in the THERM program (best cases) together with their geometric and thermal properties.

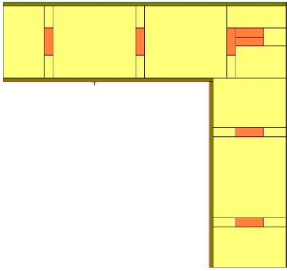
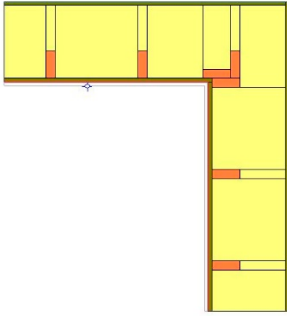
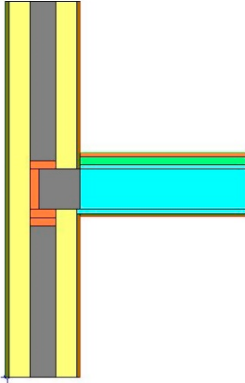
Description	Thermal Bridge Diagram	Length of the Bridge in the Building [m]	Linear Thermal Transmittance [W/(m·K)]
External corner with a timber frame located centrally in relation to wall thickness		18.12	−0.1237
External corner with a timber frame located on the inner side of the wall		18.12	−0.1153
Connection of a wall and a ceiling with a timber frame located centrally in relation to wall thickness		37.20	0.0074

Table 4. Cont.

Description	Thermal Bridge Diagram	Length of the Bridge in the Building [m]	Linear Thermal Transmittance [W/(m·K)]
Connection of a wall and a ceiling with a timber frame located on the inner side of the wall		37.20	0.0063
Connection of a roof and a knee wall with a timber frame located centrally in relation to wall thickness		20.60	−0.0379
Connection of a roof and a knee wall with a timber frame located on the inner side of the wall		20.60	−0.0255
Connection of a roof and a gable wall with a timber frame located centrally in relation to wall thickness		10.84	−0.1044
Connection of a roof and a gable wall with a timber frame located on the inner side of the wall		10.84	−0.1019

Table 4. Cont.

Description	Thermal Bridge Diagram	Length of the Bridge in the Building [m]	Linear Thermal Transmittance [W/(m·K)]
Connection of a wall and a ground floor with a timber frame located centrally in relation to the wall thickness (fragment of the model)		37.20	−0.1996
Connection of a wall and a ground floor with a timber frame located on the inner side of the wall (fragment of the model)		37.20	−0.1969
Window placement in a wall with a timber frame located centrally in relation to wall thickness		55.90 *	0.0435
Window placement in a wall with a timber frame located on the inner side of the wall		55.90 *	0.0390

\* length of the window placement thermal bridges excluding the windows facing south, presented in Table 5.

**Table 5.** Parameters of the windows facing south.

No of Windows	Size of the Window Opening [m]	Area of the Window Opening [m <sup>2</sup> ]	Length of the Thermal Bridge [m]
3	1.20 × 1.50	5.40	16.20
3	1.50 × 1.50	6.75	18.00
3	1.80 × 1.50	8.10	19.80
4	1.20 × 1.50	7.20	21.60
4	1.50 × 1.50	9.00	24.00
4	1.80 × 1.50	10.90	26.40

Many of the thermal bridges studied in the paper had reported negative linear thermal transmittance coefficient values. It is a common situation if the well-insulated joints form convex shapes and the  $\psi$  calculations include external dimensions of the partitions [27], as demanded by the methodology for preparing energy certificates in Poland [38] and recommended by the BSim simulation manual [39].

#### 2.4. Simulations

Calculations were made using the BSim dynamic simulation program (V 7.16.8.11), enabling analyses of heat transfer and energy demand in living quarters and public utility facilities based on the control volume method [39]. It was validated as a part of the work of IEA Annex 21 and 41 [40–42], providing good agreement with the measured parameters. The program was also validated in two ways by one of the authors: according to EN 15265 standard [43], and based on the measurements carried out in the climatic chambers of the Rzeszów University of Technology. The validation procedures were described in detail in [44–46].

During the simulations, nodal points with defined physical parameters (such as density, conductivity, and heat capacity) represent closed air zones and elements of a building's structure. For each air zone, a separate balance equation is created, including heat flux inflowing and outflowing through the control surface. These include transmission of solar radiation through transparent elements, heat flux generated by installation systems, or temperature differences between outdoor and indoor environments, as well as heat transported through ventilation, infiltration, or other mechanisms of air exchange between the exterior and the interior of a building. Continuous time processes are modeled by division into discrete time steps having a finite length of one hour or less.

The equation of the energy balance for the single zone (ignoring the thermal capacity of air) was as follows [39]:

$$\begin{aligned} & \theta_z \cdot \left( \sum_i \frac{A_i}{R_{si}} + \sum_j A_{wj} \cdot U_{wj} + \sum_k \psi_k \cdot l_k + v \cdot \rho \cdot c_p \cdot (n_e + \sum_m n_{zm}) \right) \\ & = \sum_i \frac{A_i}{R_{si}} \cdot \theta_s + (\sum_j A_{wj} \cdot U_{wj} + \sum_k \psi_k \cdot l_k) \cdot \theta_e + v \cdot \rho \cdot c_p \cdot (n_e \cdot \theta_e + \sum_k n_{zk} \cdot \theta_{zk}) + \Phi_{z,sol} + \Phi_{z,syst} \end{aligned} \quad (1)$$

where:

- $i$ —number of partitions enclosing the zone,
- $j$ —number of glazed elements in the partitions enclosing the zone,
- $k$ —number of thermal bridges in the partitions enclosing the zone,
- $m$ —number of zones,
- $\theta_z$ —air temperature in the zone [°C],
- $\theta_s$ —temperature of the internal surfaces of the partitions enclosing the zone [°C],
- $\theta_e$ —outside air temperature [°C],
- $A$ —area of the surfaces enclosing the zone [m<sup>2</sup>],
- $A_w$ —area of the glazed elements in the partitions enclosing the zone [m<sup>2</sup>],
- $R_{si}$ —thermal resistance on the internal surfaces of the partitions enclosing the zone [(m<sup>2</sup>·K)/W],

$U_w$ —thermal transmittance coefficient of the glazed elements in the partitions enclosing the zone [ $W/(m^2 \cdot K)$ ],  
 $\psi$ —linear thermal transmittance of the thermal bridges [ $W/(m \cdot K)$ ],  
 $l$ —length of the thermal bridges [m],  
 $v$ —air volume in the zone [ $m^3$ ],  
 $\rho$ —air density [ $kg/m^3$ ],  
 $c_p$ —specific heat of the air [ $J/(kg \cdot K)$ ],  
 $n_e$ —number of air exchanges between the zone and the external air [1/s],  
 $n_z$ —number of air exchanges between the zone and the adjacent zones [1/s],  
 $\Phi_{z,sol}$ —heat transferred to the zone by solar radiation [W],  
 $\Phi_{z,sys}$ —heat transferred to the zone by installation systems [W].

Heat transfer in the construction was treated as non-stationary, including the thermal capacity of each layer. The energy balance for each of the elements allowed for the calculation of the heat inflowing and outflowing to the adjoining elements, and the temperature change within their volume (knowing the specific heat of building materials used).

The climatic data used in simulations may come from the user's measurements and observations, or typical meteorological years (TMYs) collected according to the national procedures. The range of necessary input parameters includes air temperature, directional incident radiation, diffuse sky radiation, and relative air humidity. Wind direction and velocity might also be necessary, especially when a more accurate model of natural ventilation is needed.

The simulations used climatic data from the TMY for the Warsaw Okęcie station (latitude  $52^\circ 10' E$ , longitude  $20^\circ 58' N$ , the height of station 107 m a.s.l.). Warsaw is often considered a representative of Poland's climate because the air temperature and insolation there correspond to the average values for the entire country. The need for heating rooms in the Polish climate conditions usually appears between September and May. During that time, according to TMY, the mean external temperature was  $5.1^\circ C$ , and the monthly mean insolation on a horizontal plane was  $59.6 \text{ kWh}/m^2$ .

The modeled building was a single-family building with  $133.5 \text{ m}^2$  of usable space. It had a ground floor and a habitable attic under a sloped roof. The building was oriented in such a way that the wall opposite the entrance was facing south, and the size and the number of windows placed there were changing

External partitions were simulated in two construction variants, with a load-bearing timber frame located centrally in relation to the wall thickness or located on the inner side of the wall. All of the partitions complied with the current regulations in force in Poland, and the heat transfer coefficients were as follows:  $U = 0.20 \text{ W}/(m^2 \cdot K)$  for external walls,  $U = 0.15 \text{ W}/(m^2 \cdot K)$  for roofs,  $U = 0.30 \text{ W}/(m^2 \cdot K)$  for floors, and  $U = 0.77$  to  $0.78 \text{ W}/(m^2 \cdot K)$  for windows. The thermal bridges were modeled according to the description in Section 2.2.

The building's interior was treated as one thermal zone (excluding the space below the ridge and above the collar beams) with a heating setpoint of  $20^\circ C$ . In the building, there was gravity ventilation with an air exchange rate equal to 0.5 per hour. Internal gains were assumed as  $6.8 \text{ W}/m^2$ , as set in the methodology for preparing energy certificates in Poland [38].

For the two versions of wall construction (with the load-bearing structure located centrally in relation to the wall thickness or located on the inner side of the wall), different numbers and sizes of windows facing south were taken into account to check the influence of the thermal bridges along the window's perimeter on the total energy needs. (Table 5).

### 3. Results and Discussion

For the basic case (three windows  $1.20 \text{ m} \times 1.50 \text{ m}$  on the south wall), the energy demand calculated during the heating season excluding thermal bridges was  $39.3 \text{ kWh}/(m^2 \cdot \text{year})$ . This enabled the building to be classified as "low-energy", for which the limit of the heating demand is often presumed as  $40\text{--}50 \text{ kWh}/(m^2 \cdot \text{year})$  [47,48]. In this case, the results were

the same for both types of walls because their thermal transmittance did not differ and the modifications connected with thermal bridges were not taken into account in the analyses.

The thermal bridges were then included in the simulations by assigning the linear thermal transmittance coefficients to the specific edges in the geometry model of the building. As the majority of them had negative values of thermal transmittance, the final values of the energy need were smaller by approximately 16% compared with the base case. This may seem not obvious, but is a natural consequence of performing calculations using the external dimensions of the building, recommended by [38,39]. The results also illustrate the fact that the calculation of energy demand using external dimensions overestimates the heat losses in buildings, allowing to be on “the safe side” if thermal bridges are not taken into account in the modeling.

If the thermal bridges were included in the calculations and the load-bearing frame was placed centrally on the wall, the energy needs for heating amounted to 32.8 kWh/(m<sup>2</sup>·year). In the other case, when the frame was located on the inner side of the wall, the heating demand was slightly higher and amounted to 33.0 kWh/(m<sup>2</sup>·year). Therefore, the differences between the two analyzed variants may be considered negligible and both types of walls may be treated as solutions comparable from the point of view of the building’s heating demand.

An increment of the window height resulted in a linear decrease of the energy demand (Figure 9), as the greater solar gains prevailed over greater heat losses through the area of the windows and edge thermal bridges. The differences between energy needs in the cases with the smallest and the biggest window area were approximately 5%. In all of the analyzed cases, heating demand was slightly lower (approximately 0.7%) if the load-bearing structure was located centrally on the wall. The changes in the length of the thermal bridges with positive thermal transmittance did not cause any major effect on the thermal properties of the building as a whole, confirming the results obtained in the base case (with the smallest size of the windows).

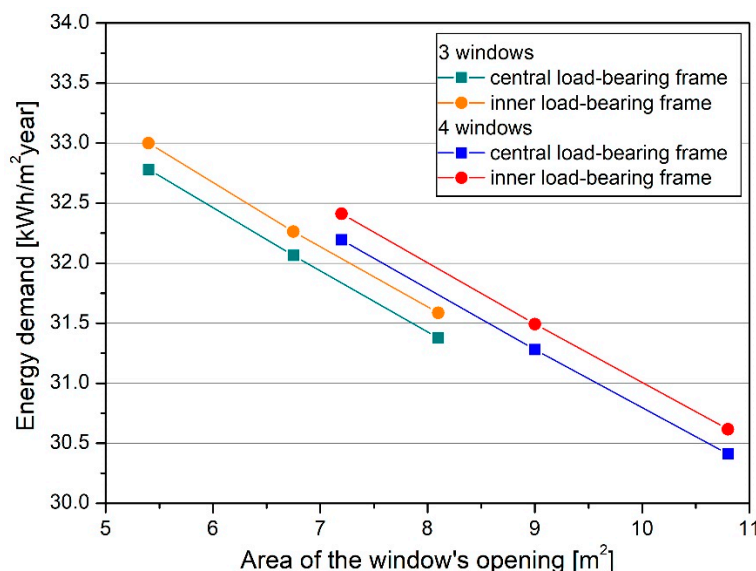


**Figure 9.** Energy demand depending on the area of the window’s opening.

For the same window area, the smaller number of openings is more beneficial from an energy point of view, as the length of the thermal bridges is smaller. Additionally, the non-glazed, composite-insulated partition is characterized by a lower heat transfer coefficient than the window, which means that heat loss is lower.

Table 6 shows the share of the thermal bridges in total heat transfer. These proportions were estimated by dividing the heat transfer coefficients of the buildings’ envelope into the parts representing the linear heat transfer through the homogenous partitions and two-dimensional heat transfer through the linear joints. As the thermal conditions inside

and outside of the building are universal, the share of the heat transfer coefficients of the particular bridges in the overall heat transfer coefficient of the buildings' casing were equal to their share in the heat losses.

**Table 6.** Share of the thermal bridges in the total heat transfer.

Thermal Bridge	Share in the Total Heat Transfer [%]	
	Timber Frame Located Centrally in Relation to Wall Thickness	Timber Frame Located on the Inner Side of the Wall
External corner	−2.5	−2.3
Connection of a wall and a ceiling	0.3	0.3
Connection of a roof and a knee wall	−0.9	−0.6
Connection of a roof and a gable wall	−2.3	−2.1
Connection of a wall and a ground floor	−8.3	−8.2
Window placement in a wall	3.5 to 3.8	3.1 to 3.3
Sum	−10.2 to −9.9	−9.8 to −9.6

The bridges representing the connection of walls and the ground floor, together with the window placement in a wall, took the biggest part of the heat transfer. It was not the longest thermal bridge (the linear bridge around the windows was longer), but it was characterized by the highest value of the linear thermal transmittance coefficient. It is worth noting, however, that it was a negative value, as opposed to the thermal transmittance around the windows. Connections of the walls and the ceiling had the smallest influence on the total heat transfer, and these bridges may be treated as negligible despite their extensive length. The nodes appearing along the roof joining the gable and knee wall have a bigger share in the total heat transfer, together with external corners.

The remaining partitions have an approximate share in the heat transfer by transmission as follows: walls—35.5%, roof—18.8%, floor on the ground—33.5%, windows—22.1%.

#### 4. Conclusions

The presented calculations allowed to for the comparison of the influence of two types of walls constructed with the load-bearing wooden frame and insulated with a hemp-lime composite on the heating demand of an exemplary building. The analyses included the thermal bridges formed along the connections of the partitions, causing some differences in the final energy needs. The negative value of the joints' heat transfer coefficients was not a sign of the inflow of heat into the building, but a consequence of the adopted assumptions concerning the dimensions of the partitions, coherent with the regulations in Poland and the modeling recommendations in the used simulation program.

The analyses showed that both types of wall construction were comparable as to the final energy demand, despite differences in the thermal quality of the bridges typical for the placing of the wooden frame inside the wall or along its inner surface. Addressing the up-to-date research on the subject, the analyses proved the important influence of thermal bridges on the thermal quality of a building's fabric. However, in this specific case, the differences between the two analyzed types of construction were negligible regarding energy demand in the building.

The studies allowed for the formulation of additional detailed conclusions, which are as follows:

- the percentage share of thermal bridges in heat loss through transmission in the analyzed building was −9.6 to −10.2;
- the greatest absolute share in heat loss through transmission had the connection between the floor on the ground and the outer wall, and the lowest absolute value had the connection between the ceiling and the wall;

- linear heat transfer coefficient of the window's placement in a wall had the biggest positive value, so this node could play the decisive role in the choice of the preferred wall type; however, it turned out that the changes in its length did not modify the trend beneficially for the walls with the central location of the timber frame;
- while maintaining a constant glazing area, it was more advantageous to minimize the number of windows, because shorter thermal bridges helped to reduce heat losses.

The building itself was classified as a low-energy one, proving the usefulness of ecological building materials and constructions in diminishing energy demand in the heating season.

The studies had some limitations, above all concerning the influence of the length of the remaining bridges (except for the window perimeter) on the energy demand or varying the insulation properties of the external partitions. This would require creating additional models of the building with different sizes of walls and roofs and different thermal properties of the materials included in the partitions. Such research is planned in the future, and it could help in a more in-depth understanding of the interactions between energy needs and building structure.

**Author Contributions:** Conceptualization, M.G. and P.B.; methodology, M.G. and P.B.; software, M.G.; validation, M.G. and P.B.; formal analysis, M.G., P.B. and M.B.; investigation, P.B.; resources, M.G. and P.B.; data curation, M.G. and P.B.; writing—original draft preparation, M.G. and P.B.; writing—review and editing, M.G., P.B., M.B. and G.Ł.; visualization, M.G. and P.B.; supervision, M.G., P.B., M.B. and G.Ł.; project administration, P.B. and G.Ł.; funding acquisition, M.B. and G.Ł. All authors have read and agreed to the published version of the manuscript.

**Funding:** This paper was prepared and partially funded within the timeframe of project Mobility FCE, Mobility CTU and with project No. SGS19/143/OHK1/3T/11 and was partially funded by the Technology Agency of the Czech Republic under project No. FW03010422.

**Data Availability Statement:** Data is contained within the article.

**Conflicts of Interest:** The authors declare that they have no conflict of interest.

## References

1. Yuan, X.; Wang, X.; Zuo, J. Renewable energy in buildings in China—A review. *Renew. Sustain. Energy Rev.* **2013**, *24*, 1–8. [CrossRef]
2. Building Performance Institute Europe (BPIE). *Renovation Strategies of Selected EU Countries. A Status Report on Compliance with Article 4 of the Energy Efficiency Directive*; BPIE: Brussels, Belgium, 2014; Available online: <http://bpie.eu/wp-content/uploads/2015/10/Renovation-Strategies-EU-BPIE-2014.pdf> (accessed on 13 October 2022).
3. Trotta, G. Assessing energy efficiency improvements, energy dependence, and CO<sub>2</sub> emissions in the European Union using a decomposition method. *Energy Effic.* **2019**, *12*, 1873–1890. [CrossRef]
4. Böhm, M.; Beránková, J.; Brich, J.; Poláček, M.; Srba, J.; Němcová, D.; Černý, R. Factors influencing envelope airtightness of lightweight timber-frame houses built in the Czech Republic in the period of 2006–2019. *Build. Environ.* **2021**, *194*, 107687. [CrossRef]
5. Bouchair, A. Steady state theoretical model of fired clay hollow bricks for enhanced external wall thermal insulation. *Build. Environ.* **2008**, *43*, 1603–1618. [CrossRef]
6. Prata, J.; Simões, N.; Tadeu, T. Heat transfer measurements of a linear thermal bridge in a wooden building corner. *Energy Build.* **2018**, *158*, 194–208. [CrossRef]
7. Šadauskienė, J.; Ramanauskas, J.; Krawczyk, D.A.; Klumbytė, E.; Fokaides, P.A. Investigation of Thermal Bridges of a New High-Performance Window Installation Using 2-D and 3-D Methodology. *Buildings* **2022**, *12*, 572. [CrossRef]
8. Bergero, S.; Cavalletti, P.; Chiari, A. Energy refurbishment in existing buildings: Thermal bridge correction according to DM 26/06/2015 limit values. *Energy Procedia* **2017**, *140*, 127–140. [CrossRef]
9. Al-Sanea, S.A.; Zedan, M.F. Effect of thermal bridges on transmission load and thermal resistance of building walls under dynamic conditions. *Appl. Energy* **2012**, *98*, 584–593. [CrossRef]
10. Asdrubali, F.; Baldinelli, G.; Bianchi, F. A quantitative methodology to evaluate thermal bridges in buildings. *Appl. Energy* **2012**, *97*, 365–373. [CrossRef]
11. Ge, H.; Baba, G. Effect of dynamic modeling of thermal bridges on the energy performance of residential buildings with high thermal mass for cold climates. *Sustain. Cities Soc.* **2017**, *34*, 250–263. [CrossRef]
12. Kim, S.; Seo, J.; Jeong, H.; Kim, J. In situ measurement of the heat loss coefficient of thermal bridges in a building envelope. *Energy Build.* **2022**, *256*, 111627. [CrossRef]

13. Kotti, S.; Teli, D.; James, P.A.B. Quantifying Thermal Bridge Effects and Assessing Retrofit Solutions in a Greek Residential Building. *Procedia Environ. Sci.* **2017**, *38*, 306–313. [[CrossRef](#)]
14. Ilomets, S.; Kuusk, K.; Paap, L.; Arumagi, E.; Kalamees, T. Impact of linear thermal bridges on thermal transmittance of renovated apartment buildings. *J. Civ. Eng. Manag.* **2017**, *23*, 96–104. [[CrossRef](#)]
15. Zhang, X.; Jung, G.-J.; Rhee, K.-N. Performance Evaluation of Thermal Bridge Reduction Method for Balcony in Apartment Buildings. *Buildings* **2022**, *12*, 63. [[CrossRef](#)]
16. Evola, G.; Margani, G.; Marletta, L. Energy and cost evaluation of thermal bridge correction in Mediterranean climate. *Energy Build.* **2011**, *43*, 2385–2393. [[CrossRef](#)]
17. Martin, K.; Erkokreka, A.; Flores, I.; Odriozola, M.; Sala, J.M. Problems in the calculation of thermal bridges in dynamic conditions. *Energy Build.* **2011**, *43*, 529–535. [[CrossRef](#)]
18. Jedidi, M.; Benjeddou, O. Effect of Thermal Bridges on the Heat Balance of Buildings. *Int. J. Civ. Eng.* **2018**, *2*, 41–49.
19. Ilomets, S.; Kalamees, T. Evaluation of the criticality of thermal bridges. *J. Build. Pathol. Rehabil.* **2016**, *1*, 11. [[CrossRef](#)]
20. Cox-Ganser, J.M. Indoor dampness and mould health effects—Ongoing questions on microbial exposures and allergic versus nonallergic mechanisms. *Clin. Exp. Allergy* **2015**, *45*, 1478–1482. [[CrossRef](#)]
21. Robertson, H.J. Spatial characteristics of southeast Australian housing linked with allergic complaint. *Build. Environ.* **2001**, *36*, 931–937. [[CrossRef](#)]
22. Coulburn, L.; Miller, W. Prevalence, Risk Factors and Impacts Related to Mould-Affected Housing: An Australian Integrative Review. *Int. J. Environ. Res. Public Health* **2022**, *19*, 1854. [[CrossRef](#)] [[PubMed](#)]
23. Johansson, S.; Balksten, K.; Strandberg-de Bruijn, P.B. Risk for Mould Growth on Hemp-Lime at Different Relative Humidity. *Constr. Technol. Archit.* **2022**, *1*, 588–594. [[CrossRef](#)]
24. Kosiachevskiy, D.; Abahri, K.; Chaouche, M.; Prat, E.; Daubresse, A.; Bousquet, C. Risk assessment of mold growth in hemp concrete. In Proceedings of the SynerCrete'18 International Conference on Interdisciplinary Approaches for Cement-based Materials and Structural Concrete, Funchal, Portugal, 24–26 October 2018.
25. Barclay, M.; Holcroft, N.; Shea, A.D. Methods to determine whole building hygrothermal performance of hemp-lime buildings. *Build. Environ.* **2014**, *80*, 204–212. [[CrossRef](#)]
26. ISO 10456:2007; Building Materials and Products. Hygrothermal Properties. Tabulated Design Values and Procedures for Determining Declared and Design Thermal Values. International Organization for Standardization: Geneva, Switzerland, 2007.
27. Brzyski, P.; Grudzińska, M.; Majerek, D. Analysis of the Occurrence of Thermal Bridges in Several Variants of Connections of the Wall and the Ground Floor in Construction Technology with the Use of a Hemp-Lime Composite. *Materials* **2019**, *12*, 2392. [[CrossRef](#)]
28. Grudzińska, M.; Brzyski, P. The Occurrence of Thermal Bridges in Hemp-Lime Construction Junctions. *Period. Polytech. Civ. Eng.* **2019**, *63*, 377–387. [[CrossRef](#)]
29. Benfratello, S. Thermal and structural properties of hemp-lime biocomposite. *Constr. Build. Mater.* **2013**, *48*, 745–754. [[CrossRef](#)]
30. Shea, A.; Lawrence, M.; Walker, P. Hygrothermal performance of an experimental hemp-lime building. *Constr. Build. Mater.* **2012**, *36*, 270–275. [[CrossRef](#)]
31. Walker, R.; Pavia, S. Moisture transfer and thermal properties of hemp-lime concretes. *Constr. Build. Mater.* **2014**, *64*, 270–276. [[CrossRef](#)]
32. Bourdot, A.; Moussa, T.; Gacoin, A.; Maalouf, C.; Vazquez, P.; Thomachot-Schneider, C.; Bliard, C.; Merabtine, A.; Lachi, M.; Douzane, O.; et al. Laboratory Characterization of a hemp-based agro-material: Influence of starch ratio and hemp shive size on physical, mechanical, and hygrothermal properties. *Energy Build.* **2017**, *153*, 501–512. [[CrossRef](#)]
33. Stevulova, N.; Kidalova, L.; Junak, J.; Cigasova, J.; Terpakova, E. Effect of hemp shive sizes on mechanical properties of lightweight fibrous composites. *Procedia Eng.* **2012**, *42*, 496–500. [[CrossRef](#)]
34. Arnaud, L.; Gourlay, E. Experimental study of parameters influencing mechanical properties of hemp concretes. *Constr. Build. Mater.* **2012**, *28*, 50–56. [[CrossRef](#)]
35. Kosiński, P.; Brzyski, P.; Tunkiewicz, M.; Suchorab, Z.; Wiśniewski, D.; Palczynski, P. Thermal Properties of Hemp Shives Used as Insulation Material in Construction Industry. *Energies* **2022**, *15*, 2461. [[CrossRef](#)]
36. ISO 10211:2017; Thermal bridges in building construction. Heat flows and surface temperatures—Detailed calculations. International Organization for Standardization: Geneva, Switzerland, 2017.
37. Mitchell, R.; Kohler, C.; Zhu, L.; Arasteh, D.; Carmody, J.; Huizenga, C.; Curcija, D. *Therm 6.3/Window 6.3 NFRC Simulation Manual*; Lawrence Berkeley National Laboratory: Berkeley, CA, USA, 2011.
38. Decree of the Minister of Infrastructure and Development from 27th February 2015 on the Methodology of Determining Energy Characteristics of Buildings or Their Parts and Energy Certificates. *J. Laws Repub. Pol.* **2015**, 376.
39. Wittchen, K.B.; Johnsen, K.; Grau, K. *B5Sim User's Guide*; Danish Building Research Institute: Hørsholm, Denmark, 2004.
40. Lomas, K.J.; Eppel, H.; Martin, C.J.; Bloomfield, D.P. *Empirical Validation of Building Energy Simulation Programs Using Test Room Data*; Volume 1: Final Report; International Energy Agency: Paris, France, 1994.
41. Woloszyn, M.; Rode, C. *Final Report Annex 41. Whole Building Heat, Air and Moisture Response*; Volume 1: Modelling Principles and Common Exercises; IEA Annex 41, Subtask 1; International Energy Agency: Paris, France, 2008.
42. Roels, S. *Final Report Annex 41. Whole Building Heat, Air and Moisture Response*; Volume 2: Experimental Analysis of Moisture Buffering; IEA Annex 41, Subtask 2; International Energy Agency: Paris, France, 2008.

43. EN 15265:2011; Thermal Performance of Buildings. Calculation of Energy Needs for Space Heating and Cooling Using Dynamic Methods. General Criteria and Validation Procedures. European Committee for Standardization: Brussels, Belgium, 2011.
44. Grudzińska, M. *Glazed Balconies as Passive Greenhouse Systems. Assessment of the Functioning in Polish Climatic Conditions*; Lublin University of Technology Publishing House: Lublin, Poland, 2020; ISBN 978-83-7947-447-9.
45. Grudzińska, M. Validation of a dynamic simulation program according to EN ISO 15265. *E3S Web Conf.* **2018**, *49*, 00040. [[CrossRef](#)]
46. Grudzińska, M. Thermal and optical properties of the sunspace casing as factors influencing temperature rise in greenhouse systems. *Materials* **2021**, *14*, 7411. [[CrossRef](#)]
47. Thullner, K. *Low-Energy Buildings in Europe-Standards, Criteria and Consequences. A Study of Nine European Countries*; Rapport TVIT-10/5019, Rapport EBD-R-10/32; Lund University: Lund, Sweden, 2010.
48. Hoyle, B. *Low-Energy Building Engineering*; English Press: Delhi, India, 2011.